Chemical Science

Cite this: *Chem. Sci.*, 2012, **3**, 1764

www.rsc.org/chemicalscience

MINIREVIEW

Graphene-based electronic sensors

Qiyuan He, Shixin Wu, Zongyou Yin and Hua Zhang*

Received 18th February 2012, Accepted 27th March 2012
DOI: 10.1039/c2sc20205k

Graphene, the archetypal two-dimensional material, is attracting increasing attention due to its unique and superior properties. The atomic thickness of the graphene sheet is extremely sensitive towards the change of local environment, making it an ideal channel material in field-effect transistors used as electronic sensors. In this minireview, we review the graphene-based electronic sensors for detection of various chemicals and biomolecules. We first introduce the different kinds of graphene materials used in the electronic sensors and how they affect the device sensing performance. Then we focus on the use of the reduced graphene oxide for the fabrication of cost-efficient, high-yield and highly reproducible sensing devices.

Introduction

Detection of chemical and biological molecules with high sensitivity and selectivity is crucial to not only a wide range of research fields, but also various practical applications, such as detection of gas leakage, diagnosis of diseases and health care, *etc.* Many sensing approaches, such as electrochemistry,[1–3] surface enhanced Raman spectroscopy (SERS)[4] and surface plasma resonance (SPR),[5] have been used to develop highly sensitive and selective, low cost sensing devices aiming at the detection of numerous toxic chemicals and in particular, biomolecules in the aqueous environment. Electronic sensors based on field-effect transistors (FETs)[6–8] are favored due to their high sensitivity, simple device configuration, low cost, miniaturization of devices, and real-time detection.

The realization of electronic detection is based on the conductance change of FET semiconducting channels upon adsorption of target molecules. This idea of detection with FETs was demonstrated by using bulk materials, such as gas-sensitive metal oxides[9] or ion-sensitive polymer membranes,[10] as channels. However, the bulk channels, used in these previously reported planar devices, restricted the interaction between target molecules and channel only on the channel surface, resulting in low sensitivity of the FET sensors. Therefore, their further applications are limited.

Semiconductor nanomaterials are an ideal solution to increase the performance of FET sensors. One-dimensional (1D) single-crystal silicon nanowires (SiNWs) is a typical example.[6,11] The high switching characteristics (ON/OFF ratio > 10^7) of SiNW-based FETs is crucial for the extremely high sensitivity of electronic sensors based on this material. Another successful example is 1D carbon nanotubes (CNTs). Individual semiconducting CNTs,[12] CNT thin films[13] and CNT arrays[14] have been employed as channels in high-performance electronic sensors. In addition, conjugated polymer thin films[15] and organic single crystals[7] have also been used as channels in some other electronic sensors.

The recently developed two-dimensional (2D) material, graphene,[16–18] is attracting increasing attention due to its wide range of electronics applications in transparent electrodes[19–24] and active material for energy harvesting[25] and storage,[26] and channel materials[27–33] for FETs. Besides the superior electronic properties, graphene offers high flexibility and biocompatibility,[34,35] large surface area and facile chemical functionalization compared to CNTs, making it an ideal sensing platform. Most importantly, the atomic thickness of graphene means all the carbon atoms directly interact with the analyte, promising an ultimate sensitivity, even superior to that of 1D Si nanowires (SiNWs) and CNTs.

In this minireview, we briefly introduce the recently developed chemical and biological electronic sensors based on graphene and its derivatives. The device structures and working principles of graphene-based field-effect transistors (GFETs) in both gas and liquid phases are demonstrated. The high-performance detection towards the small toxic gas molecules, biomolecules, and bioactivities of living cells is discussed. In addition, different kinds of graphene channels, including pristine graphene, graphene grown by the chemical vapor deposition (CVD), and reduced graphene oxide (rGO), and their effects on the device fabrication and sensing performance are discussed.

Device configuration and working principle

A typical FET consists of a semiconducting channel between two metal electrodes, the drain and source electrodes, through which the current is injected and collected. The conductance of the channel can be capacitively modulated by varying the gate potential through a thin dielectric layer,[36] typically 300 nm SiO_2.

School of Materials Science and Engineering, Nanyang Technological University, 50 Nanyang Avenue, Singapore 639798, Singapore. E-mail: HZhang@ntu.edu.sg; Web: http://www.ntu.edu.sg/home/hzhang/

In a typical p-type metal oxide semiconductor field-effect transistor (MOSFET), the negative gate potential leads to the accumulation of holes (majority charge carries), resulting in an increase of the channel conductance, while the positive gate potential leads to the depletion of holes, and hence a decrease of the conductance. In the case of the electronic sensor, the adsorption of molecules on the surface of the semiconducting channel either changes its local surface potential or directly dopes the channel, resulting in change of the FET conductance. This makes the FET a promising sensing device with easily adaptable configuration, high sensitivity and real-time capability. In some cases, the gate electrode is removed, in order to simplify the device structure, to form a chemiresistor.[37] Such configuration is suitable for fabrication of graphene-based sensors on polymer substrates for flexible electronics applications. Despite the lack of modulation by the gate potential, the working principle of the chemoresistor is same as a normal FET sensor.

As shown in Fig. 1a, in a typical gas sensing system, the channel is directly exposed to the target gas. The adsorption of gas molecules results in the doping of the semiconducting channel, leading to a conductance change of the FET device. Experiments[38,39] and theoretical[40,41] studies concluded that the charge transfer from the adsorbed gas molecules to the semiconducting channel is the dominant mechanism for the current response, which is similar to CNT-based gas sensors.[42,43] Although some studies on CNT-based gas sensors suggested that the modulation of metal–semiconductor contacts[44] might also be the dominant mechanism, most studies on graphene-based gas sensors have ruled out this possibility.

In order to detect bio-species, the GFETs should operate in an aqueous environment. As shown in Fig. 1b, the graphene channel is usually immersed in a flow cell or sensing chamber, which is used to confine the solution. The drain and source electrodes are insulated to prevent current leakage from ionic conduction. Different insulators including polydimethylsiloxane (PDMS)/silicone rubber,[30–33,45] SiO_2 thin film,[46] SU8 passivation[47–49] and silicone rubber[50] are used in different device structures. The gate electrode, usually Ag/AgCl or Pt, is immersed in the solution. The gate potential is applied through the thin electric double-layer capacitance formed at the channel–solution interface. The double-layer thickness (or Debye length) is determined by the ionic strength in the solution, typically within 1 nm, which is even thinner than the thin HfO_2 layer used in the high performance top-gate GFETs.[51] Normally, the solution-gate FET is over two orders of magnitude more sensitive than the typical back-gate FET.

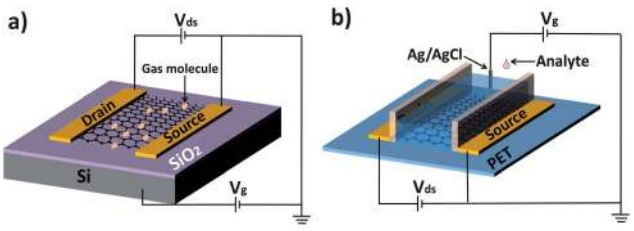

Fig. 1 (a) Typical back-gate GFET on Si/SiO_2 substrate used as gas sensor. (b) Typical solution-gate GFET on flexible polyethylene terephthalate (PET) substrate used as chemical and biological sensor in aqueous solution.

Two major sensing mechanisms have been proposed for graphene-based biosensors in solution, *i.e.* the electrostatic gating effect and the doping effect. The gating effect suggests that the charged molecules adsorbed on graphene act as an additional gating capacitance which alters the conductance of the graphene channel. On the other hand, the doping effect suggests a direct charge transfer between the adsorbed molecules and the graphene channel, similar to gas sensing. In a real case, the actual sensing mechanism might be a combination of both mechanisms, or involve more complicated mechanisms.[52,53]

Choice of graphene materials

As shown in Fig. 2, three major kinds of graphene materials are used in electronic sensors, *i.e.*, the pristine graphene prepared by the mechanical exfoliation method (Fig. 2a),[54] graphene grown by CVD process, referred to as CVD-graphene (Fig. 2b),[55] and reduced graphene oxide (rGO) obtained by the reduction of graphene oxide (GO), arising from the chemical exfoliation of graphite (Fig. 2c).[56]

Pristine graphene without any functionalization is nearly insoluble in any solvent. Therefore, the only way to produce the pristine graphene channel is to directly deposit graphene sheets onto the substrate through mechanical cleavage, known as the "scotch-tape" method.[16] This kind of graphene is incontrollable in shape, size and location. Hence the yield of devices is extremely

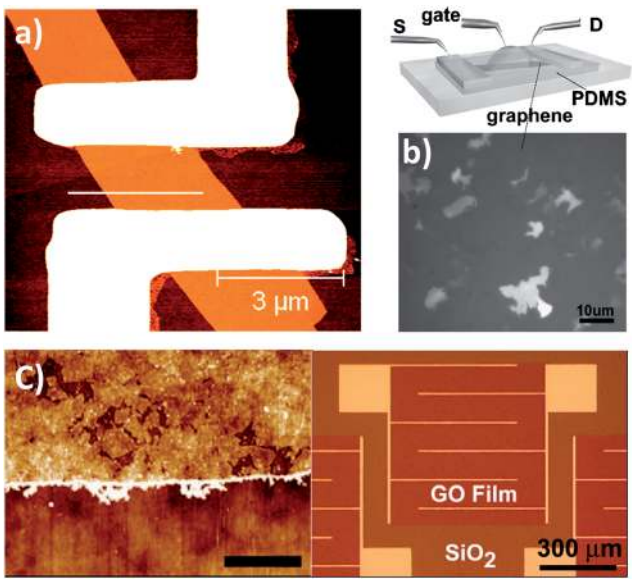

Fig. 2 Different kinds of graphene materials used in electronic sensors. (a) AFM image of a typical GFET based on the pristine graphene (thickness = 0.8 nm) obtained by mechanical cleavage, connected by Ti/Au electrodes deposited by e-beam lithography. Adapted with permission from ref. 54. (b) Optical microscopy image of CVD-graphene films and schematic illustration of the solution-gate FET. Adapted with permission from ref. 55. (c) AFM image of rGO film obtained by spin-coating (thickness = 6 nm, scale bar = 1 μm) and optical microscopy image of an electrically isolated rGO device with interdigitated Ti/Au contacts. Adapted with permission from ref. 56.

low, and such pristine graphene is more suitable only for theoretical study and proof-of-concept demonstration.

Recent development in the CVD process has led to the preparation of wafer-scale graphene film on metal substrates (such as Ni, Ru, Cu) with single-layer yield as high as 95%.[57] The high conductivity and transparency makes the CVD-graphene perfect for flexible electrodes used in optoelectronic applications. Importantly, electronic sensors can also benefit from the high-yield and high-quality CVD-graphene, which enables the mass production of devices with high reproducibility. However, since the CVD-graphene can only be produced on certain metallic substrates, it requires additional transfer steps to make devices, leading to contaminations and destruction of graphene sheets.[58] Alternatively, the epitaxial graphene[59] grown on SiC substrate, another type of thermally grown graphene at wafer-size scale, has been used for the electronic sensing applications. However, it also needs additional transfer steps for device fabrication.

The chemical exfoliation of graphite into GO opens up a new way to produce solution-processable graphene, which is important for the mass production of graphene-based electronics at low cost. A stable, homogeneous GO aqueous suspension is usually produced by a modified Hummers method.[60] Thus-prepared GO is highly oxidized and contains carboxylic acid, epoxy and alcohol groups. These functional groups on GO can be partially removed by chemical or thermal reduction to restore the π-conjugated structure and conductivity of GO in the produced rGO. Although the remaining functional groups on rGO will degrade the electronic performance by lowering its conductivity compared to the pristine graphene, the rGO-based electronic sensor may benefit from the enhanced interaction[61] or chemical reaction[62] between the remaining functional groups and the analyte.

Graphene-based gas sensors

Theoretical studies have predicted that the conduction of the graphene channel can be tuned by adsorption of gas molecules, acting as donors or acceptors, on the graphene surface.[40,61,63] Experimentally, Schedin *et al.* fabricated a gas sensor based on mechanically cleaved single-layer graphene.[64] A four-probe measurement was carried out in their experiment to eliminate the influence of contact resistance. The ultimate detection of a single NO_2 gas molecule was claimed, owing to the high carrier mobility of graphene and the extremely low noise of the device. Meanwhile, Dan *et al.* argued that the intrinsic response of graphene toward the gas adsorption was rather small, and the major device response came from the chemical contamination on graphene which not only doped the graphene channel but also enhanced the adsorption of gas molecules.[54]

The follow-up work on GFETs was mainly based on the scalable graphene, *i.e.*, CVD-graphene, epitaxial graphene and reduced graphene oxide (rGO). For example, one recent work[65] showed that three-dimensional (3D) graphene foam with few-layer graphene grown by CVD method[66,67] is able to detect NO_2 gas to an order of magnitude lower concentration compared to the commercial polypyrrole sensor (Fig. 3a). It is worth mentioning that the device fabrication with 3D graphene foam is quite scalable without the requirement of graphene transfer steps. Meanwhile, Chen *et al.* reported the direct growth of vertically oriented graphene sheets by using plasma-enhanced CVD on Au electrodes to fabricate GFET sensors for detection of NO_2 and NH_3.[68] In addition, Nomani *et al.* directly fabricated a NO_2 sensor using the epitaxial graphene on a semi-insulating 6*H*-SiC surface without any transfer step.[69]

Although gas sensors based on individual rGO sheets have been demonstrated,[70] the major advantage of rGO lies in its solution processibility, which is compatible with most thin-film technologies. Fowler *et al.* fabricated a chemoresistor sensor using rGO sheets spin-coated on an interdigitated electrode array.[39] The rGO sheets are mostly single-layer and discontinuous, connected by the electrode array. The different current responses to NO_2 and NH_3 supported the charge transfer mechanism. Since the GFET was operated at p-type region, the electron-withdrawing NO_2 would cause a decrease of resistance, while the electron-donating NH_3 would cause an increase of resistance. Moreover, this chemoresistor was able to detect 2,4-dintrotoluene (DNT), a relatively volatile component found in the trinitroluene (TNT) explosive, at the ppb level.[39]

Other different fabrication methods were used to fabricate gas sensors based on rGO thin films. Robinson *et al.* fabricated the GFET by direct deposition of Au electrodes on 2–4 nm rGO thin films obtained by spin-coating.[56] They found that the rGO-based device exhibited significantly lower noise than did the device based on CNT networks, resulting in a much lower detection limit of dinitrotoluene. Their study also revealed the different gas adsorption rates on the remaining oxygen-containing groups and the sp^2-carbon backbone of rGO.

The solution processibility of rGO makes it possible to fabricate rGO-based sensors by the commercial inkjet-printing technique,[71] where the used ink was the surfactant-protected rGO aqueous suspension obtained through a green reduction of GO by vitamin C. The rGO channels were patterned by inkjet-printing on the polyethylene terephthalate (PET) film. Sip socket leads were used to connect the rGO channels to form a flexible, lightweight sensor array. A calculated detection limit of 400 ppt for NO_2 based on the signal-to-noise ratio of 3 was demonstrated. It is worth mentioning that although the rGO film used in this study was rather thick (>100 nm) compared to other rGO sensors, it did not compromise the sensitivity of the gas sensor.

Most recently, the current dielectrophoresis method, previously used to fabricate CNT-based electronics, has been used to prepare rGO channels between drain and source electrodes to construct GFET sensors.[72] The Au electrodes were covered with CVD-graphene before the deposition of rGO film between them. The graphene coverage lowered the contact resistance between the rGO channel and metal electrodes. The rGO sheets were further functionalized with Pd nanoparticles (PdNPs) to enhance the gas sensitivity. The authors proposed that such enhancement of sensitivity arose from the switch from the symmetric Schottky barrier to an asymmetric n-type Schottky barrier at the contact between PdNPs and rGO upon the NO adsorption. This is different from the PdNP-functionalized GFET based hydrogen sensor, which took advantage of the high solubility of H_2 in PdNPs at room temperature.[73] By combining the CVD-graphene coverage on the electrodes and PdNPs functionalization on the rGO channel, the detection limit for NO gas was improved by an order of magnitude.[72]

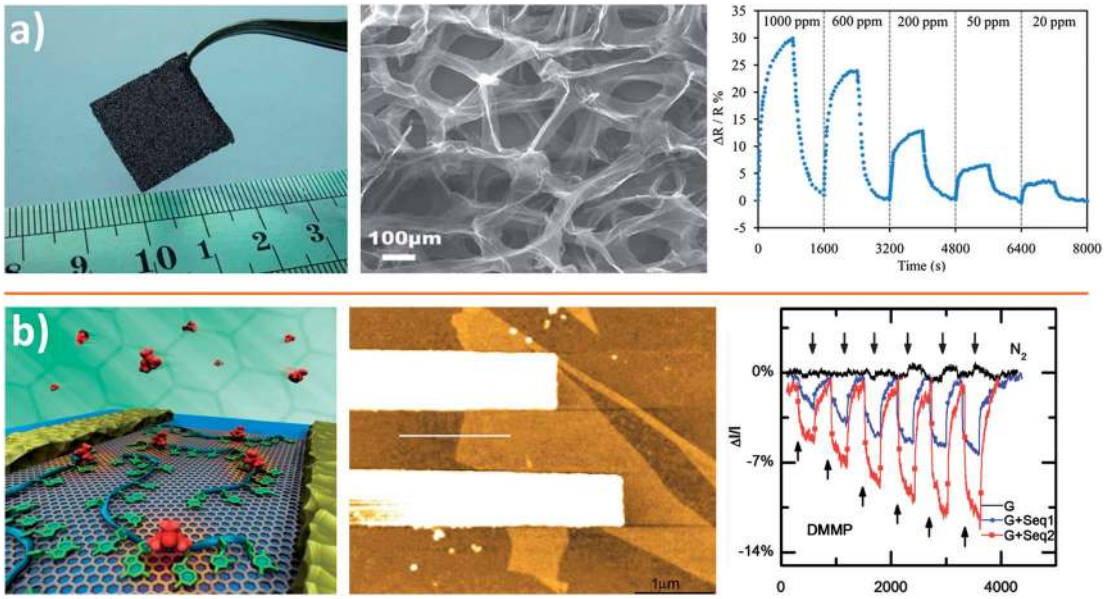

Fig. 3 (a) Photo and SEM images of 3D graphene foam grown by CVD and the real-time detection of NH_3 at different concentrations. Adapted with permission from ref. 65. (b) Schematic illustration of ssDNA adsorbed on pristine graphene as channel for gas sensing, AFM image of ssDNA adsorbed on pristine graphene between Au electrodes, and the real-time detection of dimethyl methyl phosphonate without ssDNA (black curve) and with two different sequences of ssDNA (red and blue curves). Adapted with permission from ref. 79.

Besides the commonly demonstrated NO_x and NH_3 gas sensors, GFET-based sensors were also employed in detection of H_2,[73–75] H_2O,[64,76] alcohol,[77] and H_2S.[78] Despite the excellent sensitivity of graphene-based gas sensors, challenges still remain in making practical GFET sensors. For example, their recovery time (time required to return to initial conductance after sensing) is relatively long, ranging from tens of minutes to hours. Lu *et al.* tried to solve this problem by coupling the graphene channel with single-stranded DNA (ssDNA) as a sensitizing agent.[79] As shown in Fig. 3b, the non-covalent functionalization of ssDNA acts as a concentrator of water and analyte molecules on the chemically inert and hydrophobic surface of pristine graphene, resulting in a rapid response as well as fast and complete recovery after sensing.[79] Meanwhile, another study found that the rGO-based FET showed much faster response and recovery when it was operated at n-type region, instead of the p-type region commonly used.[80] Another typical drawback of GFET sensors is device-to-device variation. In order to solve this problem, thin-film devices based on large-area, high-quality and homogenous graphene films are favored. Finally, more detailed mechanistic study is still required to further understand GFET sensors, in order to enhance their performance and reliability in practical gas sensing application.

Graphene-based pH sensors and biosensors

The large surface area, good biocompatibility and excellent chemical stability make graphene and its derivatives ideal platforms for biosensors in aqueous environment.[81] Moreover, the facile covalent or noncovalent surface functionalization makes them easy to conjugate with different receptors for specific biodetections.

The GFET was successfully used in aqueous environment as a pH sensor.[46] In this work, epitaxially grown single-, double-, triple-layer graphene sheets were used in solution-gate FETs with Ag/AgCl as the gate electrode. A positive shift of the transfer curve (drain to source current *vs.* solution-gate potential) was found when the pH value of the incubated buffer solution increased from 2 to 12. Single-, double- and triple-layer GFETs showed similar pH sensitivity at ~99 mV pH^{-1}. The sensing mechanism arises from the change of ions (OH^- and H_3O^+) adsorbed on the graphene surface at different pH value, which changed the electrochemical double layer (electrostatic gating) at the graphene–solution interface.

Interestingly, a smaller pH sensitivity of ~20 mV pH^{-1} was observed at a GFET based on mechanically exfoliated single-layer graphene suspending on two Au electrodes.[45] The suspending graphene channel was designed to reduce the noise in the electronic sensing. However, no insulation was used in their experiments, which might induce ionic leakage on the bare Au electrodes. Moreover, a similar shift of transfer curves upon the change of pH value was observed at another kind of GFET sensor,[50] where silicone rubber was used as the insulator between the Au electrode and the graphene channel. Therefore, the influence of ionic leakage from the buffer solution to electrodes was neglectable. However, the shift of transfer curve (Dirac point) was found to be unstable from device to device, making the pH measurement unreliable.[50] The reason might arise from the charged impurities adsorbed on the top of graphene surface and the interface between graphene and the underneath substrate.

Recently, a full-carbon GFET sensor array made by monolithically integrated graphene and graphite was reported.[47] The selective growth of monolithically integrated graphene channels and graphite electrodes was realized by a CVD process on a spatially patterned heterogeneous metal catalyst. The GFET array can be transferred onto various flexible substrates to form a multiplexed sensor array. A simultaneous and real-time pH

detection with 10 devices on a single sensor array was demonstrated with excellent reproducibility. Since graphene has ambipolar property, the sensor can be operated at both n-type and p-type regions by simply changing the solution-gate potential.

However, in a most recent work, Fu *et al.* argued that GFETs were insensitive to the pH value.[82] They claimed that no specific binding of any ions was anticipated in a clean graphene surface. Based on their report, the highly sensitive pH detection mentioned above is most likely due to the defects of graphene sheets. These defects, mostly the oxygen-containing groups, act as binding cites for protons, resulting in the pH response. This was further confirmed by the deliberate introduction of defects in graphene *via* mild UV-ozone treatment, which increased the pH sensitivity of the sensor.[82] Therefore, the difference in pH sensitivity (12–99 mV pH^{-1}) from the previously reported pH sensors simply reflects the difference in the quality of the graphene channel. In another study, defects were found to be induced in the graphene channel when the solution-gate potential was above +0.3 V,[83] which might further compromise the reliability of the GFET-based pH sensors.

The successful operation of GFET sensors in aqueous environment has boosted biosensing studies. For example, Li *et al.* used it as a DNA sensor.[55] In this work, millimeter-size CVD-graphene was first functionalized with Au nanoparticles (AuNPs). The thiolated probe ssDNA was then immobilized on AuNPs through thiol–Au bonding. Using the back-gate GFET, the detection of complementary target ssDNA was realized by monitoring the shift of the transfer curve before and after DNA hybridization. Similar to the gas sensor, the sensing mechanism was believed to be the direct n-doping effect of the adsorbed DNA to the graphene channel. This was confirmed by the negative shift of the transfer curve and the Dirac point. The detection limit of this DNA sensor reached the pM level with single mismatch distinction.

However, the aforementioned DNA sensor is not real-time since the GFET is operated in back-gate mode to measure the change of transfer curves. A real-time DNA sensor based on a solution-gate GFET was demonstrated by our group using an rGO thin film as the channel. In this report, the Langmuir–Blodgett method[84] was used for the scalable fabrication of high-quality rGO thin films with one- to two-layer thickness.[85] The rGO channel was functionalized with PtNPs by *in situ* photochemical reduction, to immobilize the thiolated probe ssDNA through the thiol–Pt bonding. The detection was realized by real-time monitoring of the current change upon addition of the target ssDNA. Showing no response to the mismatched ssDNA, a calculated detection limit of 2.5 nM for the complementary target ssDNA was achieved. In a different approach towards real-time DNA detection,[62] a few-layer GO film was spin-coated on patterned thin Au (10 nm) electrodes to configure a GFET sensing chip. Ethylenediamine was used before the chemical reduction of GO to protect the active binding sites and provide the primary amine groups after the reduction. These primary amine groups were used to immobilize the aminated probe ssDNA through the glutaraldehyde used as linker. The real-time detection of 10-nm target ssDNA with only minor response to mismatched DNA was demonstrated.[62]

Besides DNA, GFET sensors have been used for the real-time detection of other biomolecules such as glucose[86] and proteins.[50,52,87–89] Ohno *et al.* showed that their pH sensor[50] is capable to detect the adsorption of bovine serum albumin (BSA) in physiological buffer solution. A real-time sub-nM detection of BSA was demonstrated. The sensing mechanism was attributed to the electrostatic gating effect, which means that the negatively charged proteins adsorbed on the graphene surface acted as additional negative gating, which increased the conductance of the GFET when it was operated at p-type region. It is worth mentioning that in this study, the GFET combined the use of back gate and solution gate to study the different gating effects.

The aforementioned protein sensor is based on the non-specific adsorption of proteins on the graphene surface.[50] However, the functionalization of graphene with receptors is necessary to specifically detect target protein. For example, Ohno *et al.* functionalized GFET with immunoglobulin E (IgE) aptamers to achieve a selective detection of IgE proteins.[89] The functionalization of aptamers was realized by anchoring 1-pyrenebutanoic acid succinimidyl ester (1-pbase), a linker molecule often used to functionalize CNTs, onto the graphene surface through π–π interaction. Ethanolamine was then used to deactivate and block the remaining excess reactive groups on the graphene surface. In another example, graphene sheets obtained from the thermal expansion of graphite were functionalized with specific antibodies to selectively detect the cancer biomarker, prostate specific antigen (PSA).[52] The same linker molecule (1-pbase) was used for the functionalization, while BSA passivation was used to prevent non-specific adsorption.

Our group reported the chemical functionalization of a patterned rGO thin film with biotin to specifically detect avidin.[32] In this work, the rGO thin film was first coated with poly(ethylene imine) (PEI) and poly(ethylene glycol) (PEG). The PEI was used to immobilize the biotin (receptor) through the amine groups on its polymer backbone. PEG was then applied to prevent the non-specific adsorption of other proteins. The rGO-based sensor was able to detect avidin in the buffer solution with high sensitivity and selectivity. Moreover, the sensor has a full-rGO configuration, which means the rGO film was used as both electrodes and the semiconducting channel. The excellent flexibility of rGO made the whole device fully flexible and the device functioned well even after 5000 bending cycles. Also the solution processibility of rGO made the fabrication very cheap, and highly reliable. Another demonstration of the rGO-based protein sensor was reported by Mao *et al.*[88] As shown in Fig. 4a, a thermally reduced GO film was functionalized with AuNPs-antibody (anti-IgG) conjugates to specifically detect the target protein (IgG).[88] A blocking buffer containing fish gelatin and BSA was used to prevent non-specific adsorption. The detection was realized by a typical back-gate FET test. However, a decrease of drain to source current (I_{ds}) was observed upon adsorption of target proteins (Fig. 4a), instead of the commonly observed shift of the transfer curve in the pH[46,50] and DNA sesors.[55]

Compared to the detection of biomolecules, the detection of living cells is more challenging as the interaction between the graphene channel and living cell membranes is much more complicated. Over recent years, 1D SiNWs[6] and CNTs[13] have been extensively studied in the detection of living cells and their bioactivities. Nevertheless, graphene offers a better opportunity to study the cell–nanomaterial interface since its 2D structure

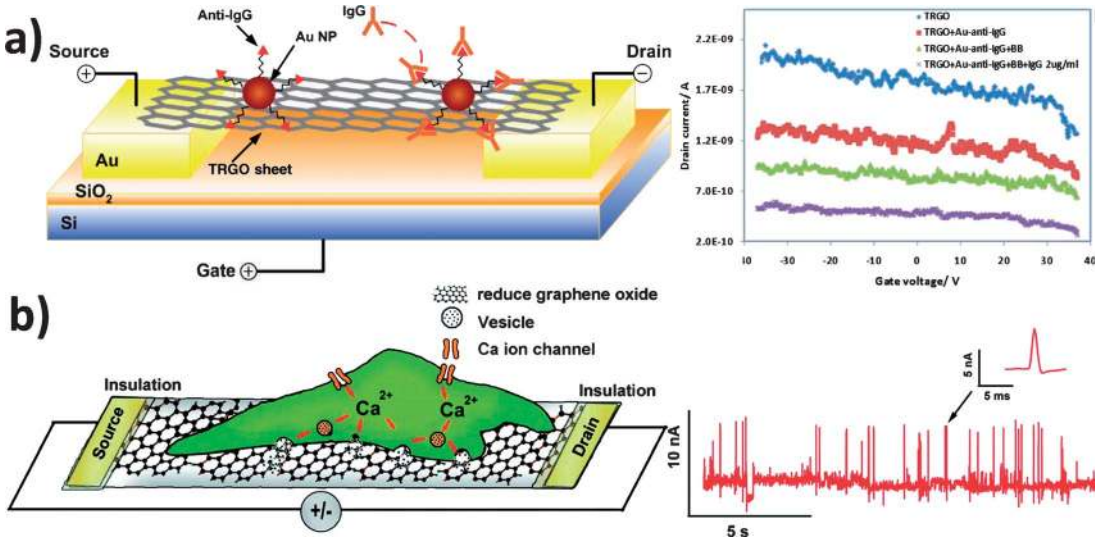

Fig. 4 (a) Schematic illustration of rGO FET based protein sensor. Anti-IgG is anchored onto the rGO surface through AuNPs and functions as a specific recognition group for IgG binding. The detection was realized by measuring the I_{ds}–V_g curve before and after adsorption of target protein. Adapted with permission from ref. 88. (b) Schematic illustration of the interface between a PC12 cell and rGO FET, and the dynamic secretion of catecholamines from PC12 cell triggered by potassium ions. The detection was realized by the real-time monitoring of I_{ds} during the dynamic secretion of catecholamines. Adapted with permission from ref. 30.

provides a homogeneous contact with the 2D cell membrane. For example, Cohen-Karni *et al.* reported a GFET sensor to detect bioelectrical signals from living chicken cells.[90] A back-gate GFET was fabricated using pristine graphene by the e-beam lithography on the SiO_2 substrate. A SiNWs FET was made alongside with the GFET to compare their sensing performances. The GFET sensor was able to detect the well-defined extracellular signals from the spontaneous beating of embryonic chicken cardiomyocyte. It showed a much better resolved signal than the normal planar device, but a lower spatial resolution than the SiNW FET due to its large contact area.[90] In another example, Ang *et al.* used a patterned CVD-graphene made by photolithography to configure a GFET sensor array in a PDMS flow cell.[48] After the functionalization of the graphene surface with CD36 receptor proteins, the sensor array was able to detect the capture and release of malaria-infected red blood cells at the single cell level. Similar work has been reported by Hess *et al.*,[49] in which a sensor array was fabricated by transfer of photolithography-patterned CVD-graphene onto a sapphire substrate pre-coated with a thermally evaporated Ti/Au electrode array. The sensor array with 16 individual GFETs was able to track the action potential of a cardiomyocyte-like HL-1 cell across the sensor array, showing a well-resolved signal.

Our group used an rGO-based solution-gate FET to investigate living cell behaviors on rGO.[30] As shown in Fig. 4b, the devices were fabricated based on large-scale micropatterned rGO thin films with a thickness of 1–3 nm. Living neuron cells (PC 12) were directly cultured on the rGO channel to obtain an intimate contact. The rGO FET was able to detect the adsorption of hormonal catecholamine molecules and those secreted from the living PC 12 cells with a high signal-to-noise ratio. Moreover, the rGO FET can be fabricated on the flexible polyethylene terephthalate (PET) substrate and function well during bending, which might be useful in complicated *in vivo* biosensing.

Most recently, Kempaiah *et al.* reported an exceptional detection of cell bioactivity based on the cell-induced mechanical deformation of the rGO channel.[53] In this study, the yeast cell was attached to the rGO channel through the chemical functionalization. An alcohol-induced shrinkage of the yeast cells resulted in the deformation of the rGO sheet, leading to a conductance decrease of the rGO channel.

Moreover, a GFET based on amine-modified rGO has been used to detect the attachment of bacteria.[91] The attachment of single bacterium induced a 42% increase of the conductance due to the p-doping effect. Such a high sensitivity can be explained by the good contact between the aminized rGO surface and the negatively-charged bacterial cell wall. In another example, the CVD-graphene channel functionalized with *E. coli* antibodies enabled a specific detection of *E. coli* bacteria in the presence of another bacterium (*Pseudomonas aeruginosa*).[92]

Graphene-based heavy-metal sensing

Besides bio-species, the capability to operate the GFET sensors in aqueous environment is also promising for the detection of metal ions in solution. A Hg^{2+} sensor has been demonstrated with a GFET based on the pristine graphene channel functionalized with alkylthiol to capture Hg^{2+} ions from solution.[93] Since this device was operated in the back gate with *ex-situ* observation of the shift of transfer curve, it is not a real-time detection. In addition, this detection based on the thiol–metal bonding is non-specific since it could be interfered with by the presence of other metal ions.

Recently, we demonstrated the specific detection of heavy metal ions by using chemically functionalized rGO micropatterns.[31] The patterned rGO channel was functionalized with metallothionein type II (MT-II) through 1-pbase used as the linker molecule. MT-II is a protein which can specifically bind to

heavy metal ions with high affinity and selectivity. This sensor was able to detect Hg^{2+} at levels as low as 1 nM (0.2 ppb) without response to other metal ions such as Mg^{2+}, Ca^{2+} or K^{+}. This sensitivity is superior to that of most fluorescence-based methods[94] and comparable to the recently published stripping voltammetry method.[95] By switching the functionalization from MT-II to calmodulin, a Ca^{2+} binding protein, the sensor was able to selectively detect Ca^{2+} among other ions. Instead of the direct gating effect of adsorbed metal ions, the current change arose from conformational change of the functionalized protein upon metal binding. Such conformational change brought the negatively charged protein closer to the graphene channel, therefore strengthening its gating effect.

Conclusions and outlook

The extensive applications of graphene-based field-effect transistors (GFETs) in chemical and biological sensing have been demonstrated. Graphene and its derivatives are particularly favoured as channel materials over other nanomaterials, such as 1D CNTs and SiNWs, in terms of lower noise ratio, facile functionalization, solution-processibility and biocompatibility. The potential of GFETs in biosensing, especially to interface with living tissues and organs, needs to be further explored. Future work might focus on how to make the low-cost, scalable and reproducible GFET sensors. Both CVD-graphene and reduced graphene oxide (rGO) are excellent active channels. In particular, the potential applications of rGO in electronic sensors and electronics are still underestimated. The solution processibility of rGO promises the mass production of highly reliable and practical electronic devices. Moreover, very limited work has been done on employing various graphene-based composites[18] as semiconducting channels in FETs and sensors. Functional composites such as graphene/polymer composites,[76] graphene/bioconjugates,[79,96] graphene/inorganic composites,[33,73,97] can offer more capabilities as well as better performance. Despite the intensive studies on carbon material (graphene and CNT) based electronic sensors, the sensing mechanism remains vague, which requires further exploration in order to better interpret the sensing behaviour and optimize the sensing performance.

Besides graphene, other two-dimensional (2D) semiconducting materials derived from transition-metal dichalcogenides are receiving increasing interest recently,[98–106] showing superior performance in many electronics applications.[100,103,104] For example, the top-gate FET based on mechanically cleaved single-layer MoS_2 showed an ON/OFF ratio exceeding 10^8 at room temperature.[100] Single-layer MoS_2 based transistors also show much better photoresponsivity than the graphene-based device.[104] Electronic sensors based on few-layer MoS_2 sheets have showed excellent sensitivity in NO detection[103] and importantly, recent work has reported how to prepare these novel 2D materials in large amounts,[101,102] which envisage a promising alternative for low-cost and high-performance electronic sensors.

Acknowledgements

This work was supported by MOE under AcRF Tier 2 (ARC 10/10, No. MOE2010-T2-1-060), Singapore National Research Foundation under CREATE programme: Nanomaterials for Energy and Water Management, and NTU under the New Initiative Fund FY 2010 (M58120031) and Start-Up Grant (M4080865.070.706022) in Singapore.

References

1 K. R. Ratinac, W. Yang, J. J. Gooding, P. Thordarson and F. Braet, *Electroanalysis*, 2011, **23**, 803–826.
2 Z. J. Wang, J. Zhang, P. Chen, X. Z. Zhou, Y. L. Yang, S. X. Wu, L. Niu, Y. Han, L. H. Wang, P. Chen, F. Boey, Q. C. Zhang, B. Liedberg and H. Zhang, *Biosens. Bioelectron.*, 2011, **26**, 3881–3886.
3 Z. J. Wang, J. Zhang, Z. Yin, S. X. Wu, D. Mandler and H. Zhang, *Nanoscale*, 2012, **4**, 2728.
4 M. E. Stewart, C. R. Anderton, L. B. Thompson, J. Maria, S. K. Gray, J. A. Rogers and R. G. Nuzzo, *Chem. Rev.*, 2008, **108**, 494–521.
5 K. A. Willets and R. P. Van Duyne, *Annu. Rev. Phys. Chem.*, 2007, **58**, 267–297.
6 F. Patolsky, G. F. Zheng and C. M. Lieber, *Anal. Chem.*, 2006, **78**, 4260–4269.
7 Y. L. Guo, G. Yu, Y and Q. Liu, *Adv. Mater.*, 2010, **22**, 4427–4447.
8 P. A. Hu, J. Zhang, L. Li, Z. L. Wang, W. O'Neill and P. Estrela, *Sensors*, 2010, **10**, 5133–5159.
9 N. Barsan and U. Weimar, *J. Phys.: Condens. Matter*, 2003, **15**, R813–R839.
10 P. T. McBride, J. Janata, P. A. Comte, S. D. Moss and C. C. Johnson, *Anal. Chim. Acta*, 1978, **101**, 239–245.
11 N. S. Ramgir, Y. Yang and M. Zacharias, *Small*, 2010, **6**, 1705–1722.
12 D. R. Kauffman and A. Star, *Chem. Soc. Rev.*, 2008, **37**, 1197–1206.
13 Q. Cao and J. A. Rogers, *Adv. Mater.*, 2009, **21**, 29–53.
14 X. Z. Zhou, F. Boey and H. Zhang, *Chem. Soc. Rev.*, 2011, **40**, 5221–5231.
15 L. M. Dai, P. Soundarrajan and T. Kim, *Pure Appl. Chem.*, 2002, **74**, 1753–1772.
16 K. S. Novoselov, A. K. Geim, S. V. Morozov, D. Jiang, Y. Zhang, S. V. Dubonos, I. V. Grigorieva and A. A. Firsov, *Science*, 2004, **306**, 666–669.
17 X. Huang, Z. Y. Yin, S. X. Wu, X. Y. Qi, Q. Y. He, Q. C. Zhang, Q. Y. Yan, F. Boey and H. Zhang, *Small*, 2011, **7**, 1876–1902.
18 X. Huang, X. Y. Qi, F. Boey and H. Zhang, *Chem. Soc. Rev.*, 2012, **41**, 666–686.
19 J. B. Wu, M. Agrawal, H. A. Becerril, Z. N. Bao, Z. F. Liu, Y. S. Chen and P. Peumans, *ACS Nano*, 2010, **4**, 43–48.
20 S. Bae, H. Kim, Y. Lee, X. Xu, J.-S. Park, Y. Zheng, J. Balakrishnan, T. Lei, H. Ri Kim, Y. I. Song, Y.-J. Kim, K. S. Kim, B. Ozyilmaz, J.-H. Ahn, B. H. Hong and S. Iijima, *Nat. Nanotechnol.*, 2010, **5**, 574–578.
21 Z. Y. Yin, S. X. Wu, X. Z. Zhou, X. Huang, Q. C. Zhang, F. Boey and H. Zhang, *Small*, 2010, **6**, 307–312.
22 Z. Y. Yin, S. Y. Sun, T. Salim, S. X. Wu, X. A. Huang, Q. Y. He, Y. M. Lam and H. Zhang, *ACS Nano*, 2010, **4**, 5263–5268.
23 S. X. Wu, Z. Y. Yin, Q. Y. He, X. A. Huang, X. Z. Zhou and H. Zhang, *J. Phys. Chem. C*, 2010, **114**, 11816–11821.
24 S. X. Wu, Z. Y. Yin, Q. Y. He, G. Lu, Q. Y. Yan and H. Zhang, *J. Phys. Chem. C*, 2011, **115**, 15973–15979.
25 Y. Q. Sun, Q. O. Wu and G. Q. Shi, *Energy Environ. Sci.*, 2011, **4**, 1113–1132.
26 M. Pumera, *Energy Environ. Sci.*, 2011, **4**, 668–674.
27 D. Reddy, L. F. Register, G. D. Carpenter and S. K. Banerjee, *J. Phys. D: Appl. Phys.*, 2011, **44**, 313001.
28 F. Schwierz, *Nat. Nanotechnol.*, 2010, **5**, 487–496.
29 M. Burghard, H. Klauk and K. Kern, *Adv. Mater.*, 2009, **21**, 2586–2600.
30 Q. Y. He, H. G. Sudibya, Z. Y. Yin, S. X. Wu, H. Li, F. Boey, W. Huang, P. Chen and H. Zhang, *ACS Nano*, 2010, **4**, 3201–3208.
31 H. G. Sudibya, Q. Y. He, H. Zhang and P. Chen, *ACS Nano*, 2011, **5**, 1990–1994.
32 Q. Y. He, S. X. Wu, S. Gao, X. H. Cao, Z. Y. Yin, H. Li, P. Chen and H. Zhang, *ACS Nano*, 2011, **5**, 5038–5044.
33 X. H. Cao, Q. Y. He, W. H. Shi, B. Li, Z. Y. Zeng, Y. M. Shi, Q. Y. Yan and H. Zhang, *Small*, 2011, **7**, 1199–1202.

34 S. Agarwal, X. Z. Zhou, F. Ye, Q. Y. He, G. C. K. Chen, J. Soo, F. Boey, H. Zhang and P. Chen, *Langmuir*, 2010, **26**, 2244–2247.
35 K. Wang, J. Ruan, H. Song, J. L. Zhang, Y. Wo, S. W. Guo and D. X. Cui, *Nanoscale Res. Lett.*, 2011, **6**, 8.
36 S. M. Sze, *Physics of Semiconductor Devices*, Wiley, New York, 1981, p. 431.
37 H. E. Katz, *Electroanalysis*, 2004, **16**, 1837–1842.
38 G. Lu, S. Park, K. Yu, R. S. Ruoff, L. E. Ocola, D. Rosenmann and J. Chen, *ACS Nano*, 2011, **5**, 1154–1164.
39 J. D. Fowler, M. J. Allen, V. C. Tung, Y. Yang, R. B. Kaner and B. H. Weiller, *ACS Nano*, 2009, **3**, 301–306.
40 T. O. Wehling, K. S. Novoselov, S. V. Morozov, E. E. Vdovin, M. I. Katsnelson, A. K. Geim and A. I. Lichtenstein, *Nano Lett.*, 2008, **8**, 173–177.
41 J. Berashevich and T. Chakraborty, *Phys. Rev. B: Condens. Matter Mater. Phys.*, 2010, **81**, 205431.
42 H. Chang, J. D. Lee, S. M. Lee and Y. H. Lee, *Appl. Phys. Lett.*, 2001, **79**, 3863–3865.
43 N. Peng, Q. Zhang, C. L. Chow, O. K. Tan and N. Marzari, *Nano Lett.*, 2009, **9**, 1626–1630.
44 T. Yamada, *Phys. Rev. B: Condens. Matter Mater. Phys.*, 2004, **69**, 125408.
45 Z. Cheng, Q. Li, Z. Li, Q. Zhou and Y. Fang, *Nano Lett.*, 2010, **10**, 1864–1868.
46 P. K. Ang, W. Chen, A. T. S. Wee and K. P. Loh, *J. Am. Chem. Soc.*, 2008, **130**, 14392–14393.
47 J.-U. Park, S. Nam, M.-S. Lee and C. M. Lieber, *Nat. Mater.*, 2011, **11**, 120.
48 P. K. Ang, A. Li, M. Jaiswal, Y. Wang, H. W. Hou, J. T. L. Thong, C. T. Lim and K. P. Loh, *Nano Lett.*, 2011, **11**, 5240–5246.
49 L. H. Hess, M. Jansen, V. Maybeck, M. V. Hauf, M. Seifert, M. Stutzmann, I. D. Sharp, A. Offenhäusser and J. A. Garrido, *Adv. Mater.*, 2011, **23**, 5045–5049.
50 Y. Ohno, K. Maehashi, Y. Yamashiro and K. Matsumoto, *Nano Lett.*, 2009, **9**, 3318–3322.
51 I. Meric, M. Y. Han, A. F. Young, B. Ozyilmaz, P. Kim and K. L. Shepard, *Nat. Nanotechnol.*, 2008, **3**, 654–659.
52 M. Yang and S. Gong, *Chem. Commun.*, 2010, **46**, 5796–5798.
53 R. Kempaiah, A. Chung and V. Maheshwari, *ACS Nano*, 2011, **5**, 6025–6031.
54 Y. P. Dan, Y. Lu, N. J. Kybert, Z. T. Luo and A. T. C. Johnson, *Nano Lett.*, 2009, **9**, 1472–1475.
55 X. Dong, Y. Shi, W. Huang, P. Chen and L. J. Li, *Adv. Mater.*, 2010, **22**, 1649–1653.
56 J. T. Robinson, F. K. Perkins, E. S. Snow, Z. Q. Wei and P. E. Sheehan, *Nano Lett.*, 2008, **8**, 3137–3140.
57 X. Li, W. Cai, J. An, S. Kim, J. Nah, D. Yang, R. Piner, A. Velamakanni, I. Jung, E. Tutuc, S. K. Banerjee, L. Colombo and R. S. Ruoff, *Science*, 2009, **324**, 1312–1314.
58 X. Liang, Z. Fu and S. Y. Chou, *Nano Lett.*, 2007, **7**, 3840–3844.
59 L. Wang, L. H. Tian, G. D. Wei, F. M. Gao, J. J. Zheng and W. Y. Yang, *J. Inorg. Mater.*, 2011, **26**, 1009–1019.
60 D. Li, M. B. Muller, S. Gilje, R. B. Kaner and G. G. Wallace, *Nat. Nanotechnol.*, 2008, **3**, 101–105.
61 Y. H. Zhang, Y. B. Chen, K. G. Zhou, C. H. Liu, J. Zeng, H. L. Zhang and Y. Peng, *Nanotechnology*, 2009, **20**, 185504.
62 R. Stine, J. T. Robinson, P. E. Sheehan and C. R. Tamanaha, *Adv. Mater.*, 2010, **22**, 5297–5300.
63 O. Leenaerts, B. Partoens and F. M. Peeters, *Phys. Rev. B: Condens. Matter Mater. Phys.*, 2008, **77**, 125416.
64 F. Schedin, A. K. Geim, S. V. Morozov, E. W. Hill, P. Blake, M. I. Katsnelson and K. S. Novoselov, *Nat. Mater.*, 2007, **6**, 652–655.
65 F. Yavari, Z. Chen, A. V. Thomas, W. Ren, H.-M. Cheng and N. Koratkar, *Sci. Rep.*, 2011, **1**, 166.
66 X. H. Cao, Y. M. Shi, W. H. Shi, G. Lu, X. Huang, Q. Y. Yan, Q. C. Zhang and H. Zhang, *Small*, 2011, **7**, 3163–3168.
67 Z. Chen, W. Ren, L. Gao, B. Liu, S. Pei and H. M. Cheng, *Nat. Mater.*, 2011, **10**, 424–428.
68 K. Yu, P. Wang, G. Lu, K.-H. Chen, Z. Bo and J. Chen, *J. Phys. Chem. Lett.*, 2011, **2**, 537–542.
69 M. W. K. Nomani, R. Shishir, M. Qazi, D. Diwan, V. B. Shields, M. G. Spencer, G. S. Tompa, N. M. Sbrockey and G. Koley, *Sens. Actuators, B*, 2010, **150**, 301–307.
70 G. H. Lu, L. E. Ocola and J. H. Chen, *Appl. Phys. Lett.*, 2009, **94**, 083111.
71 V. Dua, S. P. Surwade, S. Ammu, S. R. Agnihotra, S. Jain, K. E. Roberts, S. Park, R. S. Ruoff and S. K. Manohar, *Angew. Chem., Int. Ed.*, 2010, **49**, 2154–2157.
72 W. Li, X. Geng, Y. Guo, J. Rong, Y. Gong, L. Wu, X. Zhang, P. Li, J. Xu, G. Cheng, M. Sun and L. Liu, *ACS Nano*, 2011, **5**, 6955–6961.
73 J. L. Johnson, A. Behnam, S. J. Pearton and A. Ural, *Adv. Mater.*, 2010, **22**, 4877–4880.
74 W. Wu, Z. Liu, L. A. Jauregui, Q. Yu, R. Pillai, H. Cao, J. Bao, Y. P. Chen and S.-S. Pei, *Sens. Actuators, B*, 2010, **150**, 296–300.
75 B. H. Chu, C. F. Lo, J. Nicolosi, C. Y. Chang, V. Chen, W. Strupinski, S. J. Pearton and F. Ren, *Sens. Actuators, B*, 2011, **157**, 500–503.
76 J. Zhang, G. Shen, W. Wang, X. Zhou and S. Guo, *J. Mater. Chem.*, 2010, **20**, 10824–10828.
77 J. Yi, J. M. Lee and W. I. Park, *Sens. Actuators, B*, 2011, **155**, 264–269.
78 T. V. Cuong, V. H. Pham, J. S. Chung, E. W. Shin, D. H. Yoo, S. H. Hahn, J. S. Huh, G. H. Rue, E. J. Kim, S. H. Hur and P. A. Kohl, *Mater. Lett.*, 2010, **64**, 2479–2482.
79 Y. Lu, B. R. Goldsmith, N. J. Kybert and A. T. C. Johnson, *Appl. Phys. Lett.*, 2010, **97**, 083107.
80 G. Lu, K. Yu, L. E. Ocola and J. Chen, *Chem. Commun.*, 2011, **47**, 7761–7763.
81 Y. Liu, X. Dong and P. Chen, *Chem. Soc. Rev.*, 2012, **41**, 2283–2307.
82 W. Fu, C. Nef, O. Knopfmacher, A. Tarasov, M. Weiss, M. Calame and C. Schönenberger, *Nano Lett.*, 2011, **11**, 3597–3600.
83 J. Ristein, W. Y. Zhang, F. Speck, M. Ostler, L. Ley and T. Seyller, *J. Phys. D: Appl. Phys.*, 2010, **43**, 345303.
84 L. J. Cote, F. Kim and J. Huang, *J. Am. Chem. Soc.*, 2009, **131**, 1043–1049.
85 Z. Y. Yin, Q. Y. He, X. Huang, J. Zhang, S. X. Wu, P. Chen, G. Lu, Q. C. Zhang, Q. Y. Yan and H. Zhang, *Nanoscale*, 2012, **4**, 293–297.
86 Y. X. Huang, X. C. Dong, Y. M. Shi, C. M. Li, L. J. Li and P. Chen, *Nanoscale*, 2010, **2**, 1485–1488.
87 S. Mao, K. H. Yu, G. H. Lu and J. H. Chen, *Nano Res.*, 2011, **4**, 921–930.
88 S. Mao, G. Lu, K. Yu, Z. Bo and J. H. Chen, *Adv. Mater.*, 2010, **22**, 3521–3526.
89 Y. Ohno, K. Maehashi and K. Matsumoto, *J. Am. Chem. Soc.*, 2010, **132**, 18012–18013.
90 T. Cohen-Karni, Q. Qing, Q. Li, Y. Fang and C. M. Lieber, *Nano Lett.*, 2010, **10**, 1098–1102.
91 N. Mohanty and V. Berry, *Nano Lett.*, 2008, **8**, 4469–4476.
92 Y. Huang, X. Dong, Y. Liu, L.-J. Li and P. Chen, *J. Mater. Chem.*, 2011, **21**, 12358–12362.
93 T. Zhang, Z. Cheng, Y. Wang, Z. Li, C. Wang, Y. Li and Y. Fang, *Nano Lett.*, 2010, **10**, 4738–4741.
94 E. M. Nolan and S. J. Lippard, *J. Am. Chem. Soc.*, 2007, **129**, 5910–5918.
95 J. Gong, T. Zhou, D. Song and L. Zhang, *Sens. Actuators, B*, 2010, **150**, 491–497.
96 P. K. Ang, M. Jaiswal, C. H. Y. X. Lim, Y. Wang, J. Sankaran, A. Li, C. T. Lim, T. Wohland, O. Z. Barbaros and K. P. Loh, *ACS Nano*, 2010, **4**, 7387–7394.
97 S. Myung, A. Solanki, C. Kim, J. Park, K. S. Kim and K. B. Lee, *Adv. Mater.*, 2011, **23**, 2221–2225.
98 K. S. Novoselov, D. Jiang, F. Schedin, T. J. Booth, V. V. Khotkevich, S. V. Morozov and A. K. Geim, *Proc. Natl. Acad. Sci. U. S. A.*, 2005, **102**, 10451–10453.
99 S. Cho, N. P. Butch, J. Paglione and M. S. Fuhrer, *Nano Lett.*, 2011, **11**, 1925–1927.
100 B. Radisavljevic, A. Radenovic, J. Brivio, V. Giacometti and A. Kis, *Nat. Nanotechnol.*, 2011, **6**, 147–150.
101 Z. Zeng, Z. Yin, X. Huang, H. Li, Q. He, G. Lu, F. Boey and H. Zhang, *Angew. Chem., Int. Ed.*, 2011, **50**, 11093–11097.
102 J. N. Coleman, M. Lotya, A. O'Neill, S. D. Bergin, P. J. King, U. Khan, K. Young, A. Gaucher, S. De, R. J. Smith, I. V. Shvets, S. K. Arora, G. Stanton, H.-Y. Kim, K. Lee, G. T. Kim, G. S. Duesberg, T. Hallam, J. J. Boland, J. J. Wang, J. F. Donegan, J. C. Grunlan, G. Moriarty, A. Shmeliov, R. J. Nicholls, J. M. Perkins, E. M. Grieveson, K. Theuwissen, D. W. McComb, P. D. Nellist and V. Nicolosi, *Science*, 2011, **331**, 568–571.

103 H. Li, Z. Yin, Q. He, H. Li, X. Huang, G. Lu, D. W. H. Fam, A. I. Y. Tok, Q. Zhang and H. Zhang, *Small*, 2012, **8**, 63–67.
104 Z. Yin, H. Li, H. Li, L. Jiang, Y. Shi, Y. Sun, G. Lu, Q. Zhang, X. Chen and H. Zhang, *ACS Nano*, 2012, **6**, 74–80.
105 H. Li, G. Lu, Z. Y. Yin, Q. Y. He, H. Li, Q. Zhang and H. Zhang, *Small*, 2012, **8**, 682–686.
106 S. X. Wu, Z. Y. Zeng, Q. Y. He, Z. J. Wang, S. J. Wang, Y. P. Du, Z. Y. Yin, X. P. Sun, W. Chen and H. Zhang, *Small*, 2012, DOI: 10.1002/smll.201200044.